Establishment of *FUT8* Knockout Chinese Hamster Ovary Cells: An Ideal Host Cell Line for Producing Completely Defucosylated Antibodies With Enhanced Antibody-Dependent Cellular Cytotoxicity

Naoko Yamane-Ohnuki, Satoko Kinoshita, Miho Inoue-Urakubo, Machi Kusunoki, Shigeru Iida, Ryosuke Nakano, Masako Wakitani, Rinpei Niwa, Mikiko Sakurada, Kazuhisa Uchida, Kenya Shitara, Mitsuo Satoh

Tokyo Research Laboratories, Kyowa Hakko Kogyo Co., Ltd., 3-6-6 Asahi-machi, Machida-shi, Tokyo 194-8533, Japan; telephone: 81-42-725-2556; fax: 81-42-725-8330; e-mail: msatoh@kyowa.co.jp

Received 18 December 2003; accepted 29 March 2004

Published online 6 August 2004 in Wiley InterScience (www.interscience.wiley.com). DOI: 10.1002/bit.20151

Abstract: To generate industrially applicable new host cell lines for antibody production with optimizing antibody-dependent cellular cytotoxicity (ADCC) we disrupted both *FUT8* alleles in a Chinese hamster ovary (CHO)/DG44 cell line by sequential homologous recombination. *FUT8* encodes an α-1,6-fucosyltransferase that catalyzes the transfer of fucose from GDP-fucose to *N*-acetylglucosamine (GlcNAc) in an α-1,6 linkage. *FUT8*$^{-/-}$ cell lines have morphology and growth kinetics similar to those of the parent, and produce completely defucosylated recombinant antibodies. *FUT8*$^{-/-}$-produced chimeric anti-CD20 IgG1 shows the same level of antigen-binding activity and complement-dependent cytotoxicity (CDC) as the *FUT8*$^{+/+}$-produced, comparable antibody, Rituxan. In contrast, *FUT8*$^{-/-}$-produced anti-CD20 IgG1 strongly binds to human Fcγ-receptor IIIa (FcγRIIIa) and dramatically enhances ADCC to approximately 100-fold that of Rituxan. Our results demonstrate that *FUT8*$^{-/-}$ cells are ideal host cell lines to stably produce completely defucosylated high-ADCC antibodies with fixed quality and efficacy for therapeutic use. © 2004 Wiley Periodicals, Inc.

Keywords: Chinese hamster ovary (CHO) cells; *FUT8*; knockout; α-1,6-fucosylation; therapeutic antibody; antibody-dependent cellular cytoxicity (ADCC)

INTRODUCTION

Antibody-dependent cellular cytotoxicity (ADCC), a lytic attack on antibody-targeted cells, is considered one of the major immunologic mechanisms in tumor cell eradication (Cartron et al., 2002). ADCC is induced by binding of the antibody constant region (Fc) to lymphocyte receptors (FcγRs) (Clynes et al., 2000). IgG1 has two N-linked oligosaccharide chains bound to the Fc region Asn297. The N-linked oligosaccharides generally found in human serum IgG are of the complex bianntenary type, composed of a trimannosyl core structure with the presence or absence of core fucose, bisecting *N*-acetylglucosamine (GlcNAc) and terminal galactose, giving rise to structural heterogeneity (Rademacher et al., 1986). Recently, we demonstrated that ADCC is controlled almost solely by the absence of fucose on IgG1, and that galactose and bisecting GlcNAc contribute little or nothing to ADCC (Shinkawa et al., 2003). Shields et al. (2002) also reported that the improvement of FcγRIIIa binding to defucosylated IgG1 caused greatly enhanced ADCC (Shields et al., 2002). Thus, IgG1 defucosylation is a powerful and elegant mechanism to improve antibody effector function. However, no production system for completely defucosylated therapeutic antibodies is available.

Chinese hamster ovary (CHO) cell lines are one of the most universal hosts in biopharmaceutical production. CHO cells have several advantages for use in industry: high growth rate; high productivity; ease of genetic manipulation; good proliferation in large-scale suspension culture; and adaptability to protein-free media. A number of approved therapeutic antibodies are produced in CHO cells, including Rituxan and Herceptin, both of which are being used increasingly in the treatment of non-Hodgkin lymphoma (Leget and Czuczman, 1998) and breast cancer (Hortobagyi, 2001), respectively. However, the major form of N-linked oligosaccharides on CHO-produced antibodies are fucosylated, and the ADCC of such antibodies is much lower than the corresponding defucosylated antibodies (Shields et al., 2002; Shinkawa et al., 2003).

In mammals, almost all antibody fucose residues are attached to the innermost GlcNAc residue of N-linked oligosaccharides via an α-1,6 linkage (Miyoshi et al., 1997). α-1,6-fucosyltransferase catalyzes the transfer of fucose from GDP-fucose to the GlcNAc residue in an α-1,6 linkage in the medial Golgi cisternae (Longmore and Schachter, 1982; Wilson et al., 1976). *FUT8* (Hayashi et al., 2000; Javaud et al., 2000; Uozumi et al., 1996; Yanagidani et al.,

Correspondence to: M. Satoh

1997) encodes an α-1,6-fucosyltransferase gene, and no isoforms have yet been cloned. We reported recently that rat hybridoma YB2/0 cells, which produce large amounts of defucosylated recombinant antibodies, express a more than tenfold lower level of *FUT8* transcripts than CHO cells. We also showed that overexpression of *FUT8* in YB2/0 cells rescues its α-1,6-fucosylation activity, rendering it equivalent to that of CHO cells. Thus, we focused on *FUT8* and reasoned that the elimination of its function would convert CHO cells to efficient host cells for production of completely defucosylated antibodies.

Our goal was to generate stable host cell lines that produce completely defucosylated antibodies under commercially applicable conditions. For this purpose, complete and irreversible inactivation of FUT8 function in CHO cells was essential. The only way to carry this out was by gene targeting, which is well known to be an extremely rare event in somatic cells (Hanson and Sedivy, 1995). In this study we report our success in the targeted disruption of both *FUT8* alleles in CHO/DG44 cells by homologous recombination technology. The results show that $FUT8^{-/-}$ cell lines express completely defucosylated recombinant IgG1s with over two orders of magnitude higher ADCC than equivalent IgG1 produced by the parent without measurable changes in antigen binding or complement-dependent cytotoxicity (CDC).

MATERIALS AND METHODS

Cell Lines

CHO/DG44 cells, in which the dihydrofolate reductase (*DHFR*) gene locus is deleted, were obtained from Drs. Lawrence Chasin and Gail Urlaub Chasin, Columbia University, New York (Urlaub et al., 1986).

Antibodies

Rituxan was purchased from Genentech, Inc. (South San Francisco, CA)/IDEC Pharmaceuticals (San Diego, CA). YB2/0-produced chimeric anti-CD20 IgG1 was obtained as described previously (Shinkawa et al., 2003).

Hybridoma cells producing murine anti-CCR4 monoclonal antibody KM2160 were established by immunizing mice with a peptide corresponding to 2 to 29 amino acid residues of human CCR4 (Imai et al., 1998). The heavy- and light-chain variable region cDNAs of KM2160 were cloned into the chimeric IgG1 antibody expression vector pKANTEX93 (Nakamura et al., 2000). Chimeric anti-CCR4 IgG1 was expressed in CHO/DG44 cells or YB2/0 cells and purified as described previously (Shinkawa et al., 2003).

Isolation of Chinese Hamster *FUT8* cDNA

Total RNA was isolated from CHO/DG44 cells using the RNeasy Mini Kit (Qiagen, Hilden, Germany) and reverse-transcribed with oligo-dT using a Superscript first-strand synthesis system for reverse transcript–polymerase chain reaction (RT-PCR) (Invitrogen, Carlsbad, CA). A Chinese hamster *FUT8* cDNA was amplified from single-stranded CHO/DG44 cell cDNAs by PCR using primers 5′-GTCTGAAGCATTATGTGTTGAAGC-3′ and 5′-GTGAGTACATTCATTGTACTGTG-3′, designed from the murine *FUT8* cDNA (Hayashi, 2000).

Targeting Construct of *FUT8* Locus

The targeted disruption of the *FUT8* gene in CHO/DG44 cells was carried out using two replacement vectors, pKOFUT8Neo and pKOFUT8Puro. The 9.0-kb fragment of the *FUT8* gene including the first coding exon was isolated by screening the CHO-K1 cell λ-genomic library (Stratagene, La Jolla, CA) with the Chinese hamster *FUT8* cDNA as a probe to establish the targeting constructs. A 234-bp segment containing the translation initiation site was replaced with the neomycin-resistance gene (Neo^r) cassette or the puromycin-resistance gene ($Puro^r$) cassette from plasmid pKOSelectNeo or pKOSelectPuro (Lexicon, TX), respectively, flanked by *loxP* sites (Fig. 1). The diphtheria toxin gene (*DT*) cassette from plasmid pKOSelectDT (Lexicon) was inserted at the 5′ homologous region. The resulting targeting constructs, pKOFUT8Neo and pKOFUT8Puro, included the 1.5-kb 5′ homologous sequence and the 5.3-kb 3′ homologous sequence. Before transfection, the targeting constructs were linearized at a unique *Sal*I site.

Transfection and Screening for Homologous Recombinants

Subconfluent CHO/DG44 cells (1.6×10^6) were electroporated with 4 μg of linearized pKOFUT8Neo at 350 V and 250 μF using a Bio-Rad GenePulser II. After electroporation, transfectants were selected with 600 μg/mL G418 (Nacalai Tesque, Kyoto, Japan). Genomic PCR was performed in 96-well plates by the modified microextraction method reported previously (Ramirez-Solis et al., 1992) using the following primers: 5′-CTTGTGTGACTCTTAACTCTCAGAG-3′ and 5′-GAGGCCACTTGTGTAGCGCCAAGTG-3′. Homologous recombinants were identified by the 1.7-kb fragment obtained using genomic PCR and confirmed by Southern blot analysis using the 221-bp fragment amplified with the following primers: 5′-GTGAGTCCATGGCTGTCACTG-3′ and 5′-CCTGACTTGGCTATTCTCAG-3′ (Fig. 2). The hemizygous clone was subject to a second round of homologous recombination using linearized pKOFUT8Puro and drug selection with 15 μg/mL puromycin (Sigma-Aldrich, St. Louis, MO) as described earlier. The identified homozygous disruptants were electroporated with the Cre-recombinase expression vector pBS185 (Invitrogen) to remove drug-resistance gene cassettes from both *FUT8* alleles.

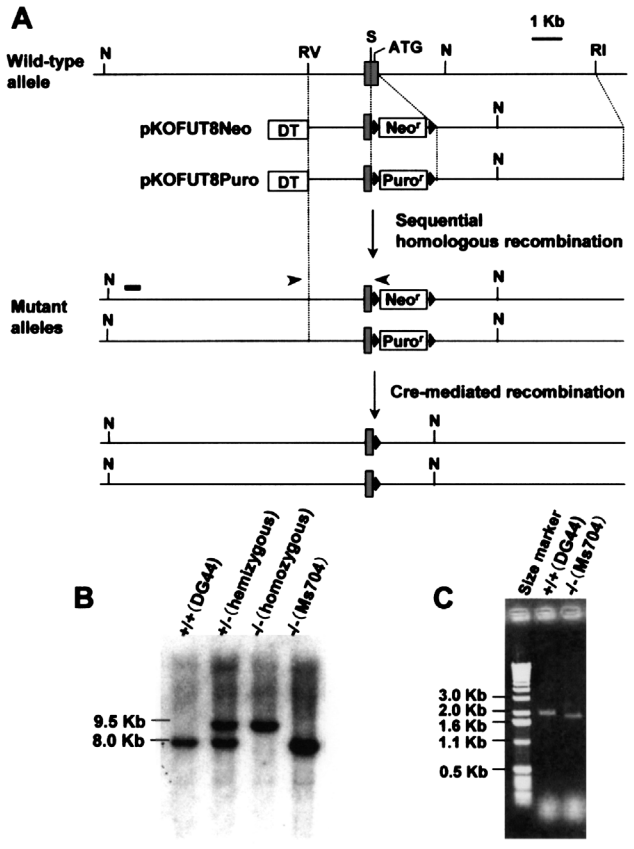

Figure 1. Strategy for targeted disruption of *FUT8* alleles in CHO/DG44 cells. (**A**) *FUT8* alleles and targeting constructs. Exon 2 (■) was modified by replacing a 234-bp segment containing the translation initiation site with the drug-resistance gene cassette, flanked by two *loxP* sites (▲). Arrowheads represent the primers for genomic PCR. The bar indicates a probe for Southern blot analysis. After sequential targeting, the drug-resistance gene cassettes were removed from both *FUT8* alleles by transient expression of Cre-recombinase. (**B**) Southern blot analysis of the parental, $FUT8^{+/-}$ and $FUT8^{-/-}$ CHO cells. Ten micrograms of genomic DNA digested with *Nhe*I was electrophoresed on a 0.6% agarose gel. (**C**) RT-PCR analysis of *FUT8* in the parental and $FUT8^{-/-}$ CHO cells. Single-stranded cDNAs prepared from each cell are subject to PCR using the primers to amplify full-length cDNAs of Chinese hamster *FUT8*.

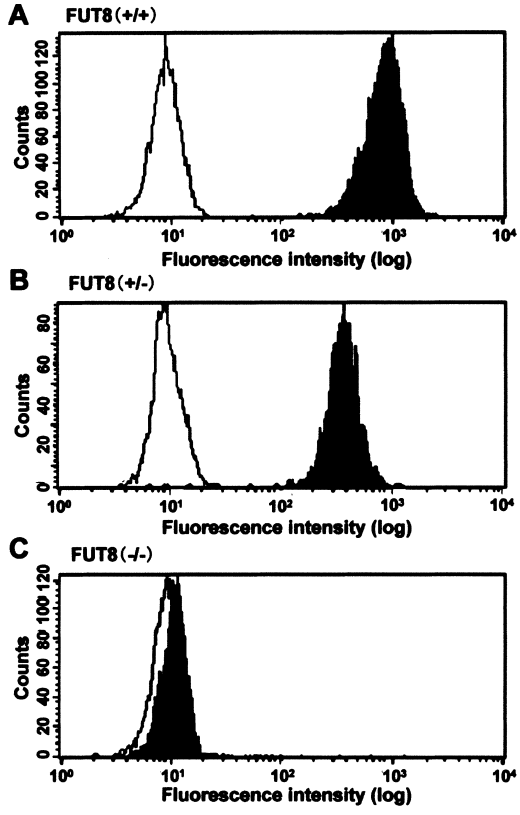

Figure 2. LCA reactivity of CHO cells. Cells were stained with FITC-labeled LCA or FITC-labeled streptavidin and analyzed by FACS. (**A**) CHO/DG44 cells. (**B**) $FUT8^{+/-}$ cells. (**C**) $FUT8^{-/-}$ cells Ms704.

Monoclonal Antibody Production by $FUT8^{-/-}$ Cells

$FUT8^{-/-}$ cell lines were electroporated with either the mouse/human chimeric anti-CD20 IgG1 (Shinkawa et al., 2003) or chimeric anti-CCR4 IgG1 expression vector and selected in media lacking hypoxanthine and thymidine. The confluent transfectants were cultured in Ex-Cell 301 Medium (JRH Biosciences, Lenexa, KS) for 1 week. IgG1 was purified from culture supernatants using MabSelect (Amersham Biosciences, Piscataway, NJ).

LCA Reactivity Analysis

Cells (2×10^5) were suspended in 50 μL of phosphate-buffered saline (PBS) containing 1% bovine serum albumin (BSA) and either 2 μg/mL fluorescein isothiocyanate (FITC)-labeled *Lens culinaris* agglutinin (LCA; Vector Laboratories, Burlingame, CA) or a 1/100 dilution of FITC-labeled streptavidin (KPL, Gaithersburg, MD) were added. After incubation at 4°C for 30 min, 1×10^4 stained cells were analyzed by FACScalibur (BD Biosciences, San Jose, CA).

IgG1 N-Linked Oligosaccharide Analysis

Fluorescence-labeled oligosaccharides were prepared from 100 μg of IgG1 by hydrazinolysis and pyridylamination, and analyzed by reverse-phase HPLC as described previously (Shinkawa et al., 2003). IgG1 monosaccharide composition was characterized by modified high-performance anion-exchange chromatography (HPAEC) analysis as previously reported (Shinkawa et al., 2003).

CD20 Binding Enzyme-Linked Immunoassay (ELISA)

Human B-lymphoma Raji-cell microsomal fraction (0.5 μg/well; JCRB CCL86) was coated onto 96-well immunoplates and incubated overnight at 4°C. Various antibody concentrations were added to the wells and incubated for 2 h at room temperature. Antibody binding to CD20 was detected by a 1/3000 dilution of goat anti-human IgG1 (H&L) peroxidase-conjugated polyclonal antibody (American Qualex, San Clemente, CA) and developed with 2,2′-azinobis(3-ethylbenzothiazoline-6-sulfonic acid)diammonium salt (ABTS).

FcγRIIIa Binding Assay

Human Phe158 FcγRIIIa cDNA (Peltz et al., 1989) was modified by replacing the transmembrane and intracellular domains with a hexa-His tag, and then subcloned into the mammalian cell expression vector pKANTEX93 (Nakamura et al., 2000). The modified FcγRIIIa was expressed in YB2/0 cells and purified from culture supernatant using Ni-NTA chromatography (Qiagen). A 1:50 dilution of goat anti-human IgG1 (H&L) polyclonal antibody (American Qualex) was coated onto 96-well immunoplates and incubated overnight at 4°C. Sample antibodies (0.5 μg/well) were added and incubated for 1 h at room temperature. The purified FcγRIIIa–His fusion protein (0.5 μg/well) was bound to samples for 1 h at room temperature. Receptor binding was detected by a 1:1000 dilution of Penta-His horseradish peroxidase (HRP) conjugate (Qiagen) and developed with 3,3′,5,5′-tetramethylbenzidine (TMB) liquid substrate system for ELISA (Sigma-Aldrich).

CDC Assay

Human B-lymphoma Ramos cells (5×10^4; ATCC CRL1596), 0.5 dilution of human serum complement (Sigma-Aldrich), and various antibody concentrations were incubated in 96-well flat-bottomed plates for 2 h at 37°C. WST-1 (15 μL; Roche Diagnostics, Basel, Switzerland) was added and incubated for 5 h at 37°C. Absorbance at 450 nm was measured and expressed as relative fluorescence units (RFU), reflecting viable cell density. Percent CDC was calculated according to the formula: %CDC activity = 100 × (RFU background − RFU test)/RFU background.

ADCC Assay

An anti-CCR4 antibody ADCC assay was performed by the lactate dehydrogenase (LDH) release assay using human peripheral blood mononuclear cells (PBMC) prepared from healthy donors by Lymphoprep (Axis Shield, Dundee, UK). Aliquots of target cells, murine T-cell lymphoma CCR4/EL4 cells expressing human CCR4 (15), were distributed into 96-well U-bottomed plates (1×10^4/50 μL) and incubated with serial dilutions of antibodies (50 μL) in the presence of human effector cells (100 μL) at an E:T ratio of 20:1. After 4-h incubation at 37°C, the supernatant LDH activity was measured using a nonradioactive cytotoxicity assay kit (Promega). Percent specific cytolysis was calculated according to the formula: %specific lysis = $100 \times (E - S_E - S_T)/(M - S_E)$ where E is the experimental release (supernatant activity from target cells incubated with antibody and effector cells), S_E is the spontaneous release in the presence of effector cells (supernatant activity from target cells incubated with effector cells), S_T is the spontaneous release of target cells (supernatant activity from target cells incubated with medium alone), and M is the maximum release of target cells (activity released from target cells lysed with 9% Triton X-100).

An ADCC assay for the anti-CD20 antibodies was performed using Raji cells and human PBMC at an E:T ratio of 20:1 as described previously (Shinkawa et al., 2003).

RESULTS

Targeted Disruption of *FUT8* Alleles

Wild-type *FUT8* alleles in CHO/DG44 cells were sequentially disrupted by homologous recombination using two targeting constructs (Fig. 1A). To enrich targeted clones, a positive–negative selection strategy was applied. Both targeting constructs contained the modified exon by replacing the translation initiation site with the drug-resistance gene, and the *DT* gene to exclude randomly integrated nonhomologous recombinants.

In the first round of gene targeting, pKOFUT8Neo was electroporated into approximately 1.0×10^8 CHO/DG44 cells. Targeted insertion of the vector, reported to be common in murine embryonic stem (ES) cells (Hasty and Bradley, 1993), did not occur. However, most of the genomic PCR-positive clones were nontargeted integrants in which the introducing vector sequence had been extended by duplication of the targeted chromosomal sequence and then integrated elsewhere in the genome (Adair et al., 1989; Aratani et al., 1992; Nairn et al., 1993; Penningon and Wilson, 1991; Scheerer and Adair, 1994). Among the 41 PCR-positive clones, only 1 was identified as a homologous recombinant by Southern blot analysis. As shown in Figure 1B, the targeted convertant gave a wild-type allele-specific fragment (8.0 kb) and a recombinant allele-specific fragment (9.5 kb) at a ratio of 1:1, suggesting that there were two *FUT8* loci on the targeted clone genome and that replacement occurred at one locus.

To disrupt the remaining wild-type allele, pKOFUT8-Puro was introduced into 1.6×10^8 $FUT8^{+/-}$ cells. Approximately 70,000 transfectants were subjected to the screening to find that the second targeted disruption occurred in 10 clones, carrying the Neo^r construct on one allele and the $Puro^r$ construct on the other, although >45,000 clones are required to identify only one hemiyzygous disruptant. In homozygous convertants, Southern blot analysis showed that a single band of the recombinant allele-specific fragment appeared and the wild-type allele-specific fragment disappeared (Fig. 1B). To exclude the drug-resistance genes from both alleles, Cre-recombinase was transiently expressed in three of the homozygous convertants, selected on the basis of good proliferation character, resulting in the generation of the $FUT8^{-/-}$ clones, Ms704, MS705, and Ms709 (Fig. 1B). All these double knockout clones were viable and exhibited morphology and growth kinetics similar to the parent.

RT-PCR analysis revealed that a mutant *FUT8* transcript with deletion of approximately 200 bp was synthesized in the $FUT8^{-/-}$ clones, whereas full-length transcript was expressed in the parent (Fig. 1C), suggesting that the

translation initiation sites of both *FUT8* alleles were deleted in the $FUT8^{-/-}$ clones.

N-Linked Oligosaccharides in *FUT8* Double Knockout Cells

To elucidate the change of α-1,6 fucosylation on oligosaccharides by disruption of the *FUT8* alleles, we analyzed the reactivity of the $FUT8^{-/-}$ clones against LCA, which recognizes the α-1,6-fucosylated trimannosyl-core structure of N-linked oligosaccharides. FACS analysis revealed that none of the $FUT8^{-/-}$ cell lines were sensitive to LCA (Fig. 2C), whereas a high concentration of LCA was bound to the parent (Fig. 2A). On the other hand, the $FUT8^{+/-}$ cells showed a slight change in LCA sensitivity from the parent (Fig. 2B). Thus, hemizygous disruption is not enough to reduce α-1,6 fucosylation sufficiently, and the lesion of both *FUT8* alleles was necessary to completely abolish fucosylation.

Chimeric anti-CD20 IgG1 Rituxan, an approved therapeutic antibody, is commercially produced in CHO/DG44 cells (Chu and Robinson, 2001). To investigate the N-linked oligosaccharide structure of $FUT8^{-/-}$-produced glycoproteins, we used chimeric anti-CD20 IgG1 expressed in $FUT8^{-/-}$ cell lines as a model. An anti-CD20 IgG1 expression vector, encoding the V region amino acid sequence of Rituxan, was introduced into $FUT8^{-/-}$ cell lines. The $FUT8^{-/-}$-produced anti-CD20 IgG1 was purified from the 1-week culture supernatant in which >80% of cells had died. Typical oligosaccharide elution profiles of fluorescence-labeled $FUT8^{-/-}$-produced IgG1 and Rituxan are compared in Figure 3. In Rituxan, most oligosaccharides (96%) were fucosylated and a few (4%) were defucosylated (Fig. 3A). In contrast, fucosylated oligosaccharides were not observed in $FUT8^{-/-}$-produced IgG1 (Fig. 3B). The monosaccharide composition of IgG1s was analyzed to confirm the fucose content change.

$FUT8^{-/-}$-produced IgG1 contained no detectable fucose residues (Fig. 4B), whereas an evident fucose peak was observed on Rituxan (Fig. 4A). In these antibodies, no difference of monosaccharide content was observed, except for fucose. We also expressed chimeric anti-CCR4 IgG1 and anti-ganglioside GD3 IgG1 in $FUT8^{-/-}$ cells, and detected no fucosylated oligosaccharide in either case (data not shown).

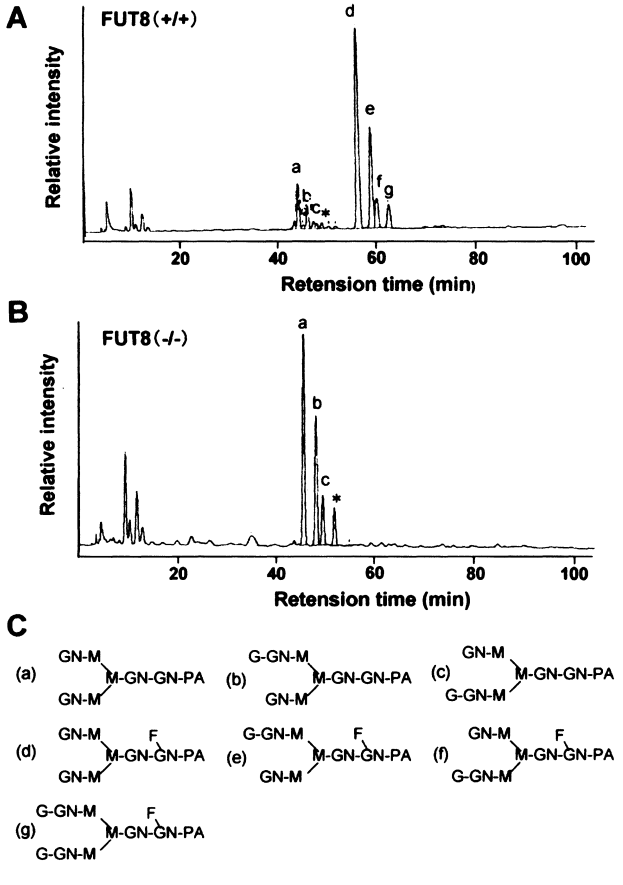

Figure 3. Oligosaccharide profiles of chimeric anti-CD20 IgG1. Oligosaccharides were prepared from Rituxan (**A**) and $FUT8^{-/-}$ (Ms704)-produced IgG1 (**B**) and pyridylaminated to be developed by reverse-phase HPLC. The alphabetical peak codes correspond to those of oligosaccharide structure in (**C**). Insets show structures associated with the peaks. GN, *N*-acetylglucosamine; G, galactose; M, mannose; F, fucose. Peaks indicated with asterisks are artifacts of pyridylamino derivatives.

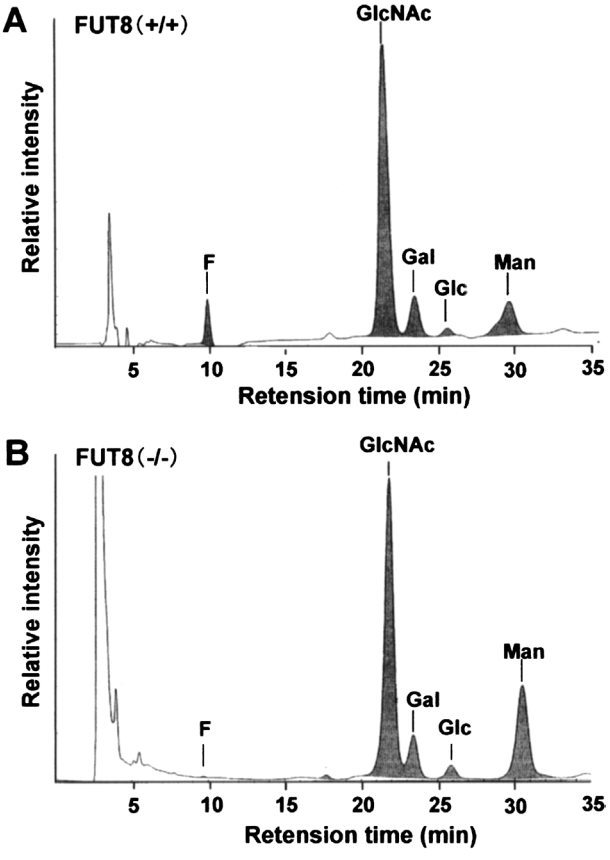

Figure 4. Monosaccharide profiles of chimeric anti-CD20 IgG1. Monosaccharides, released from Rituxan (**A**) and $FUT8^{-/-}$ (Ms704)-produced IgG1 (**B**), were hydrolyzed and subject to HPAEC analysis. Insets show structures associated with the peaks. GlcNAc, *N*-acetylglucosamine; Gal, galactose; Man, mannose; F, fucose.

These findings indicated that the *FUT8*$^{-/-}$ cells have no α-1,6-fucosylation activity and produce completely defucosylated antibodies.

In Vitro Activity of Defucosylated IgG1

We examined in vitro activity of the *FUT8*$^{-/-}$-produced IgG1s to verify the effect of completely defucosylated antibodies on therapeutic efficacy. *FUT8*$^{-/-}$-produced anti-CD20 IgG1 bound CD20-positive cell membrane with an activity similar to that of Rituxan (Fig. 5A) and showed the same CDC, CD20-positive complement-mediated cell killing (Fig. 5B). Conversely, ADCC of *FUT8*$^{-/-}$-produced IgG1 was greatly enhanced compared with Rituxan (Fig. 5C). Furthermore, *FUT8*$^{-/-}$-produced IgG1 exhibited higher ADCC than rat hybridoma YB2/0-produced IgG1 (44% defucosylated), with ADCC superior to CHO-produced IgG1 (Shinkawa et al., 2003).

Next, we studied *FUT8*$^{-/-}$-produced IgG1 binding to human FcγRIIIa with Phe158, which has a lower affinity for the Fc region than that with Val158 (Koene et al., 1997). *FUT8*$^{-/-}$-produced IgG1 exhibited significantly stronger binding activity for FcγRIIIa than Rituxan, and showed higher affinity than YB2/0-produced IgG1 (Fig. 5D).

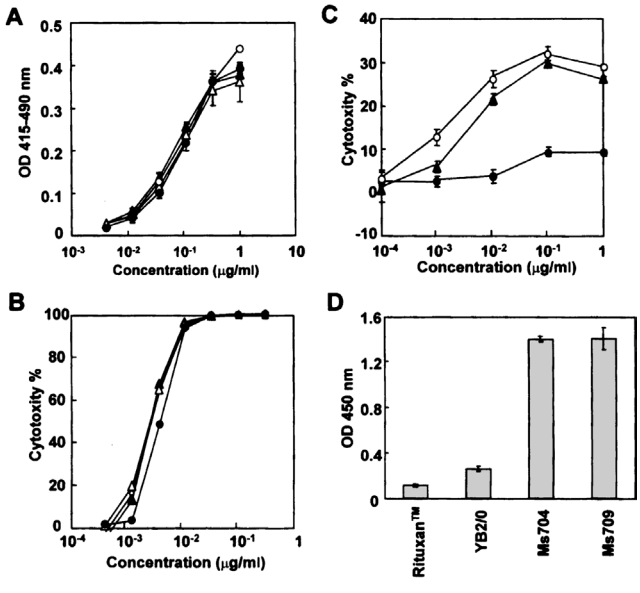

Figure 5. In vitro activity of chimeric anti-CD20 IgG1. (**A**) Raji microsomes were coated and incubated with various antibody concentrations. CD20 binding was detected by goat anti-human IgG1 polyclonal antibodies. (**B**) Lysis of Ramos human B lymphoma by human serum complement in the presence of various antibody concentrations was detected by WST-1. (**C**) Lysis of Raji human B lymphoma by human PBMC at a target:effector ratio of 1:25 in the presence of different antibody concentrations was quantified by detecting lactate dehydrogenase activity. (**D**) Goat anti-human IgG1 polyclonal antibodies were coated and incubated with equal amounts of sample antibodies and FcγRIIIa–His fusion protein. The binding was detected by anti-His-conjugated antibodies. (●) Rituxan; (●) CHO-produced IgG1; (▲) YB2/0-produced IgG1; (○) *FUT8*$^{-/-}$-produced IgG1 (Ms704); (△) *FUT8*$^{-/-}$-produced IgG1 (Ms709).

The results of ADCC assay of chimeric anti-CCR4 IgG1 supported the preceding observations. All the *FUT8*$^{-/-}$-produced anti-CCR4 IgG1 induced greatly enhanced ADCC compared with *FUT8*$^{+/+}$-produced IgG1, with much improved FcγRIIIa binding (data not shown).

These findings suggest that completely defucosylated IgG1 increases FcγRIIIa binding, thus increasing ADCC without changing either antigen binding or CDC.

DISCUSSION

In this study we established new host cells for the production of completely defucosylated antibodies. Recently, Shields et al. (2002) and our group (Shinkawa et al., 2003) reported the importance of IgG1 defucosylation on ADCC. Anti-HER2 IgG1 (21% fucosylated) produced by Lec13 cells, a CHO variant with reduction of GDP-fucose synthesis, showed 53-fold stronger FcγRIIIa binding than normal CHO-produced IgG1 (98% fucosylated) (Shields et al., 2002). Anti-IL-5 receptor IgG1 (34% defucosylated) and anti-CD20 IgG1 (91% defucosylated) produced by YB2/0 cells, with a low level of *FUT8* expression, exhibited >50-fold higher ADCC than CHO-produced IgG1s (6% to 9% defucosylated) (Shinkawa et al., 2003). However, neither Lec13 cells nor YB2/0 cells produce completely defucosylated antibodies.

Gene targeting in mammalian somatic cells is difficult to achieve and requires exceedingly laborious and time-consuming processes. The difficulty is due to the fact that, in somatic cells, nonhomologous recombination occurs several orders of magnitude more frequently than homologous recombination (Sedivy and Sharp, 1989). In general, homologous recombination in somatic cells is estimated to occur with more than 100-fold lower frequency than in ES cells (Arbones et al., 1994; Hanson and Sedivy, 1995). Nevertheless, targeted disruption is the most reliable and effective way to completely remove gene function. Other tools of loss of function, for instance, antisense, Ribozyme, and RNAi, reduce, but do not eliminate, target function.

This is the first report of the establishment of CHO double knockout cell lines obtained by targeted disruption of both alleles. Although gene targeting in CHO cells has been reported previously, the target gene variation is very limited. Only four genes, *APRT* (Adair et al., 1989; Aratani et al., 1992; Nairn et al., 1993; Penningon and Wilson, 1991; Scheerer and Adair, 1994), *DHFR* (Zheng and Wilson, 1990), *EF-2* (Kido et al., 1991), and *ERCC1* (Rolig et al., 1997), have been modified. In all these cases, only one targeting process was undertaken, either because hemizygous mutants were applied or the replacement of one allele was sufficient. In general, gene targeting in CHO cells is precluded without phenotypic selection strategies to accomplish high enrichment of targeted clones.

In the case of CHO cells, two additional obstacles further complicate gene targeting. First, the targeting vector frequently copies the target sequence on the CHO genome (Adair et al., 1989; Nairn et al., 1993; Penningon and

Wilson, 1991). The truncated end of the vector sequence is extended for several kilobases beyond the target homologous region on the vector (Aratani et al., 1992; Scheerer and Adair, 1994), and randomly integrated elsewhere on the genome. This event gives rise to many pseudo-homologous recombinants with the same sequence on nontarget and target loci. Such recombinants cannot be distinguished from true homologous recombinants by genomic PCR. In fact, we screened a very large number of transfectants, approximately 120,000, for targeted recombination of both *FUT8* alleles, because Southern blot analysis showed almost all PCR-positive clones to be vector extension integrants. Second, chromosomal abnormalities, which significantly affect the copynumber and chromosome location of the target loci (Prouty et al., 1993), have been found to accumulate in CHO cells (Siciliano et al., 1985; Warner, 1999). Most cultured somatic cell lines are aneuploid and lose native chromosome morphology because of chromosomal rearrangement during long cultivation. Assuming that several rounds of gene targeting would be necessary, we designed loxed targeting constructs in which the drug-selection gene cassettes can be removed. The clone identified with the first disruption fortunately had only two genomic *FUT8* gene copies (Fig. 1B). Thus, only two rounds of targeting were required to inactivate *FUT8* gene function.

Hemizygous disruption of the *FUT8* allele is not sufficient to reduce α-1,6 fucosylation. $FUT8^{+/-}$ cells showed a slight change in LCA sensitivity compared with the parent (Fig. 2B). $FUT8^{+/-}$-produced anti-CCR4 IgG1 exhibited few changes in fucosylation and a slight ADCC improvement (data not shown). The finding that α-1,6-fucosyltransferase activity does not correlate with *FUT8* gene dosage in CHO cells may be interpreted two ways. One possibility is that expression of *FUT8* from only one allele is phenotypically sufficient in CHO cells. The other is that the *FUT8* gene is a "functional hemizygous" (Siminovitch, 1985); the *FUT8* alleles on the CHO genome may differentially contribute to the phenotype, or either allele may be inactivated. To clarify which mechanism is correct, further studies are required.

FUT8 is the sole gene responsible for α-1,6-fucosyltransferase activity in CHO cells. In $FUT8^{-/-}$ cells, cell surface α-1,6 fucosylation disappeared (Fig. 2C), and recombinant IgG1s were completely defucosylated (Figs. 3 and 4), suggesting loss of all α-1,6-fucosyltransferase activity. *FUT8* is the only successfully cloned mammalian gene encoding an α-1,6-fucosyltransferase (Uozumi et al., 1996; Yanagidani et al., 1997), although several studies have assumed the existence of other α-1,6-fucosyltransferase gene families (Kaminska et al., 1998; Miyoshi et al., 1997; Struppe and Staudacher, 2000). Our results suggest that the *FUT8* gene is not redundant in mammals.

ADCC of $FUT8^{-/-}$-produced IgG1s was improved by more than two orders of magnitude compared with $FUT8^{+/+}$-produced IgG1s. $FUT8^{-/-}$-produced anti-CD20 IgG1 and anti-CCR4 IgG1 exhibited >100-fold (Fig. 5C) and 1000-fold (data not shown) higher ADCC, respectively, without a change in antigen-binding activity. The differing improvement in ADCC between the two antibodies may be due to cell lysis efficiency closely related to the type of antigen. Moreover, $FUT8^{-/-}$-produced IgG1 (100% defucosylated) increased ADCC much more than YB2/0-produced IgG1 (44% defucosylated). $FUT8^{-/-}$-produced IgG1s bound to FcγRIIIa with significantly more strength than YB2/0-produced IgG1, suggesting that the affinity of FcγRIIIa for the Fc region is directly related to IgG1 defucosylation (Fig. 5D). The mechanism for improvement of FcγRIIIa binding with antibody defucosylation is still an open question. There is no specific interaction between fucose and other amino acid residues on the Fc (Krapp et al., 2003). In the crystal structure of the FcγRIIIb–IgG1 Fc complex, the fucose residue has been shown to have no contact with the receptor (Radaev et al., 2001). However, our study using completely defucosylated antibodies has provided direct evidence that defucosylation plays a critical role in the improvement of FcγRIIIa binding to greatly elevate ADCC, strongly suggesting that antibody defucosylation could contribute to conformational change of the CH2 region, attached to the oligosaccharides, to enhance FcγRIIIa binding.

$FUT8^{-/-}$-produced anti-CD20 IgG1 shows the same CDC as Rituxan (Fig. 5B), demonstrating that complete defucosylation does not affect CDC. CDC, a complement-mediated lysis of target cells, is one of the major effector functions of antibodies. It is induced by two types of complement activation cascades, the classical or alternative pathways, both of which are influenced by N-linked oligosaccharide structure of the Fc region (Boyd et al., 1995; Jefferis et al., 1998; Tsuchiya et al., 1989). A previous study using Lec13-produced IgG1 reported that fucose did not contribute to C1q binding, the first step in the classical CDC pathway (Shields et al., 2002). We confirmed that IgG1 defucosylation does not reduce CDC.

Elimination of α-1,6-fucosylation activity does not affect cell viability, growth, and protein productivity. *FUT8* is highly expressed in various human cancer cell lines (Miyoshi et al., 1997). The level of α-1,6-fucosylation in N-linked oligosaccharides is known to be elevated along with carcinogenesis in mammalian liver and ovary (Noda et al., 1998a, 1998b; Takahashi et al., 2000). Hence, we had concern about the impact of disruption of the *FUT8* alleles on proliferation of CHO cells in which a high level of *FUT8* expression is observed (Miyoshi et al., 1999; Shinkawa et al., 2003). Contrary to our concerns, $FUT8^{-/-}$ cells are viable and have growth kinetics and morphologies similar to the parent CHO/DG44 cells. We expressed several types of IgG1s in $FUT8^{-/-}$ cells and found that all antibodies have normal antigen binding and enhanced ADCC, and that there is no observable difference in productivity from the parent. In addition, we carried out fed-batch suspension cultures using these cell lines and observed no change of defucosylation, with specific productivity rate comparable to that of the parent (data

not shown). Most importantly, no N-linked glycosylation change, except for defucosylation, was observed in all cases. Shields et al. noted that Lec13 cells showed lower antibody productivity than the parent, and concluded that a Lec13-type fucosylation-deficient cell line is impractical for protein production. However, we suggest that the *FUT8*$^{-/-}$ CHO/DG44 cell lines are suitable for biopharmaceutical production.

In this study, we succeeded in the targeted disruption of both *FUT8* alleles in CHO/DG44 cells in the generation of new host cells for production of completely defucosylated antibodies. *FUT8*$^{-/-}$-produced IgG1s exhibited over two orders of magnitude higher ADCC than *FUT8*$^{+/+}$-produced IgG1s. Several in vivo and clinical studies (Anolik et al., 2003; Cartron et al., 2002; Clynes et al., 2000) have proven that ADCC is one of the essential therapeutic mechanisms of antibodies, including Rituxan and Herceptin. *FUT8*$^{-/-}$ cell lines are expected to achieve both improved efficacy and reduction of dose and cost. Moreover, *FUT8*$^{-/-}$ cell lines have the great advantage of providing uniformity to biopharmaceutical N-linked glycosylation. *FUT8*$^{-/-}$ CHO/DG44 cell lines, the ideal host cells to stably produce high-ADCC therapeutic antibodies, are now available.

The authors thank Dr. Lawrence Chasin and Dr. Gail Urlaub Chasin for their generous gifts of the cell lines. We also thank Dr. Susan Lehnhardt for helpful suggestions and critical reading of the manuscript.

References

Adair GM, Nairn RS, Wilson JH, Seidman MM, Brotherman KA, MacKinnon C, Scheerer JB. 1989. Inhibitory Fc receptors modulate *in vivo* cytotoxicity against tumor targets. Proc Natl Acad Sci USA 86:4574–4578.

Aratani Y, Okazaki R, Koyama H. 1992. End extension repair of introduced targeting vectors mediated by homologous recombination in mammalian cells. Nucl Acids Res 20:4795–4801.

Arbones ML, Austin HA, Capon DJ, Greenburg G. 1994. Gene targeting in normal somatic cells: inactivation of the interferon-γ receptor in myoblasts. Nat Genet 6:90–97.

Anolik JH, Campbell D, Felgar RE, Young F, Sanz I, Rosenblatt J, Looney RJ. 2003. The relationship of FcγRIIIa genotype to degree of B cell depletion by rituximab in the treatment of systemic lupus erythematosus. Arthritis Rheum 48:455–459.

Boyd PN, Lines AC, Patel AK. 1995. The effect of the removal of sialic acid, galactose and total carbohydrate on the functional activity of Campath-1H. Mol Immunol 32:1311–1318.

Cartron G, Dacheux L, Salles G, Solal-Celigny P, Bardos P, Colombat P, Watier H. 2002. Therapeutic activity of humanized anti-CD20 monoclonal antibody and polymorphism in IgG Fc receptor FcγRIIIa gene. Blood 99:754–758.

Chu L, Robinson DK. 2001. Industrial choices for protein production by large-scale cell culture. Curr Opin Biotechnol 12:180–187.

Clynes RA, Towers TL, Presta LG, Ravetch JV. 2000. Inhibitory Fc receptors modulate *in vivo* cytotoxicity against tumor targets. Nat Med 6:443–446.

Hanson KD, Sedivy JM. 1995. Analysis of biological selections for high-efficiency gene targeting. Mol Cell Biol 15:45–51.

Hasty P, Bradley A. 1993. Gene targeting vectors for mammalian cells. In: Joyner AL, editor. Gene targeting. New York: Oxford University Press. p 1–31.

Hayashi H, Yoneda A, Asada M, Ikekita M, Imamura T. 2000. Molecular cloning of mouse alpha-1,6-fucosyltransferase and expression of its mRNA in the developing cerebrum. DNA Seq 11:91–96.

Hortobagyi GN. 2001. Overview of treatment results with trastuzumab (Herceptin) in metastatic breast cancer. Semin Oncol 28:43–47.

Imai T, Nagira M, Takagi S, Kakizaki M, Nishimura M, Wang J, Gray PW, Matsushima K, Yoshie O. 1998. Selective recruitment of CCR4-bearing Th2 cells toward antigen-presenting cells by the CC chemokines thymus and activation-regulated chemokine and macrophage-derived chemokine. Int Immunol 11:81–88.

Javaud C, Dupuy F, Maftah A, Michalski J-C, Oriol R, Petit J-M, Julien R. 2000. Ancestral exonic organization of *FUT8*, the gene encoding the α6-fucosyltransferase, reveals successive peptide domains which suggest a particular three-dimensional core structure for the α6-fucosyltransferase family. Mol Biol Evol 17:1661–1672.

Jefferis R, Lund J, Pound JD. 1998. IgG-Fc-mediated effector functions: molecular definition of interaction sites for effector ligands and the role of glycosylation. Immunol Rev 163:59–76.

Kaminska J, Glick MC, Koscielak J. 1998. Purification and characterization of GDP-L-FUC:*N*-acetyl β-D-glucosaminide α1?6 fucosyltransferase from human blood platelets. Glycoconj J 15:783–788.

Kido M, Miwatani H, Kohno K, Uchida T, Okada Y. 1991. Targeted introduction of a diphtheria toxin-resistant point mutation into the chromosomal EF-2 locus by *in vivo* homologous recombination. Cell Struct Funct 16:447–453.

Koene HR, Kleijer M, Algra J, Roos D, von dem Borne AE, de Haas M. 1997. Fc gammaRIIIa-158V/F polymorphism influences the binding of IgG by natural killer cell Fc gammaRIIIa, independently of the Fc gammaRIIIa-48L/R/H phenotype. Blood 90:1109–1114.

Krapp S, Mimura Y, Jefferis R, Huber R, Sondermann D. 2003. Structural analysis of human IgG–Fc glycoforms reveals a correlation between glycosylation and structural integrity. J Mol Biol 325:979–989.

Leget GA, Czuczman MS. 1998. Use of rituximab, the new FDA-approved antibody. Curr Opin Oncol 10:548–551.

Longmore GD, Schachter H. 1982. Product-identification and substrate specificity studies of the GDP-L-fucose:2-acetamide-2-deoxy-β-D-glucoside (Fuc-Asn-linked GlcNAc) 6-α -L-fucosyltransferase in a Golgi-rich fraction from porcine liver. Carbohydr Res 100:365–392.

Miyoshi E, Uozumi N, Noda K, Hayashi N, Hori M, Taniguchi N. 1997. Expression of α1-6-fucosyltransferase in rat tissues and human cancer cell lines. Int J Cancer 72:1117–1121.

Miyoshi E, Noda K, Yamaguchi Y, Inoue S, Ikeda Y, Wang W, Ko JH, Uozumi N, Li W, Taniguchi N. 1999. The α1-6-fucosyltransferase gene and its biological significance. Biochim Biophys Acta 1473:9–20.

Nairn RS, Adair GM, Porter T, Pennington SL, Smith DG, Wilson JH, Seidman MM. 1993. Targeting vector configuration and method of gene transfer influence targeted correction of the *APRT* gene in Chinese hamster ovary cells. Somat Cell Mol Genet 19:363–375.

Nakamura K, Tanaka Y, Fujino I, Hirayama N, Shitara K, Hanai N. 2000. Dissection and optimization of immune effector functions of humanized anti-ganglioside GM2 monoclonal antibody. Mol Immunol 37:1035–1046.

Noda K, Miyoshi E, Uozumi N, Gao C-X, Suzuki K, Hayashi N, Hori M, Taniguchi N. 1998a. High expression of α-1-6 fucosyltransferase during rat hepatocarcinogenesis. Int J Cancer 75:444–450.

Noda K, Miyoshi E, Uozumi N, Yanagidani S, Ikeda Y, Gao C, Suzuki K, Yoshihara H, Yoshikawa K, Kawano K, Hayashi N, Hori M, Taniguchi N, Yoshikawa M. 1998b. Gene expression of α1-6 fucosyltransferase in human hepatoma tissues: a possible implication for increased fucosylation of alpha-fetoprotein. Hepatology 28:944–952.

Peltz GA, Grundy HO, Lebo RV, Yssel H, Barsh GS, Moore KW. 1989. Human Fc gamma RIII: cloning, expression, and identification of the chromosomal locus of two Fc receptors for IgG. Proc Natl Acad USA 86:1013–1017.

Pennington SL, Wilson JH. 1991. Gene targeting in Chinese hamster ovary cell is conservative. Proc Natl Acad Sci USA 88:9498–9502.

Prouty SM, Hanson KD, Boyle AL, Brown JR, Shichiri M, Follansbee MR, Kang W, Sedivy JM. 1993. A cell culture model system for

genetic analysis of the cell cycle by targeted homologous recombination. Oncogene 8:899–907.

Radaev S, Motyka S, Fridman W, Sautes-Fridman C, Sun PD. 2001. The structure of a human type III Fcγreceptor in complex with Fc. J Biol Chem 276:16469–16477.

Rademacher TW, Homans SW, Parekh RB, Dwek RA. 1986. Immunoglobulin G as a glycoprotein. Biochem Soc Symp 51:131–148.

Ramirez-Solis R, Rivera-Perez J, Wallace JD, Wims M, Zheng H, Bradley A. 1992. Genomic DNA microextraction: a method to screen numerous samples. Anal Biochem 201:331–335.

Rolig RL, Layher SK, Santi B, Adair G.M., Gu F, Rainbow AJ, Nairn RS. 1997. Survival, mutagenesis, and host cell reactivation in a Chinese hamster ovary cell *ERCC1* knock-out mutant. Mutagenesis 12: 277–283.

Scheerer JB, Adair GM. 1994. Homology dependence of targeted recombination at the Chinese hamster *APRT* locus. Mol Cell Biol 14:6663–6673.

Sedivy JM, Sharp PA. 1989. Positive genetic selection for gene disruption in mammalian cells by homologous recombination. Proc Natl Acad Sci USA 86:227–231.

Shields RL, Lai J, Keck R, O'Connell LY, Hong K, Meng YG, Weikert SH, Presta LG. 2002. Lack of fucose on human IgG1 N-linked oligosaccharide improves binding to human Fcgamma RIII and antibody-dependent cellular toxicity. J Biol Chem 277:26733–26740.

Shinkawa T, Nakamura K, Yamane N, Shoji-Hosaka E, Kanda Y, Sakurada M, Uchida K, Anazawa H, Satoh M, Yamasaki M, Hanai N, Shitara K. 2003. The absence of fucose but not the presence of galactose or bisecting *N*-acetylglucosamine of human IgG1 complex-type oligosaccharides shows the critical role of enhancing antibody-dependent cellular cytotoxicity. J Biol Chem 278:3466–3473.

Siciliano MJ, Stallings RL, Adair GM. 1985. The genetic map of the Chinese hamster and the genetic consequences of chromosomal rearrangements in CHO cells. In: Gottesman MM, editor. Molecular cell genetics. New York: Wiley. p 95–135.

Siminovitch L. 1985. Mechanisms of genetic variation in Chinese hamster ovary cells. In: Gottesman MM, editor. Molecular cell genetics. New York: Wiley. p 869–879.

Struppe E, Staudacher E. 2000. Occurrence of GDP-L-fucose: β-*N*-acetylglucosamine (Fuc to Asn-linked GlcNAc) α1,6-fucosyltransferases in porcine, sheep, bovine, rabbit and chicken tissues. Biochim Biophys Acta 1475:360–368.

Takahashi T, Ikeda Y, Miyoshi E, Yaginuma Y, Ishikawa M, Taniguchi N. 2000. α1,6 fucosyltransferase is highly and specifically expressed in human ovarian serious adenocarcinomas. Int J Cancer 88:914–919.

Tsuchiya N, Endo T, Matsuta K, Yoshinoya S, Aikawa T, Kosuge E, Takeuchi F, Miyamoto T, Kobata A. 1989. Effects of galactose depletion from oligosaccharide chains on immunological activities of human IgG. J Rheumatol 16:285–290.

Uozumi N, Yanagidani S, Miyoshi E, Ihara Y, Sakuma T, Gao CX, Teshima T, Fujii S, Shiba T, Taniguchi N. 1996. Purification and cDNA cloning of porcine brain GDP-L-Fuc:*N*-acetyl-β-D-glucosaminide α1?6fucosyltransferase. J Biol Chem 271:27810–27817.

Urlaub G, Mitchell PJ, Kas E, Chasin LA, Funanage VL, Myoda TT, Hamlin J. 1986. Effect of gamma rays at the dihydrofolate reductase locus: deletions and inversions. Somat Cell Mol Genet 12:555–566.

Warner TG. 1999. Enhancing therapeutic glycoprotein production in Chinese hamster ovary cells by metabolic engineering endogenous gene control with antisense DNA and gene targeting. Glycobiology 9:841–850.

Wilson JR, Williams D, Schachter H. 1976. The control of glycoprotein synthesis: *N*-acetylglucosamine linkage to a mannose residue as a signal of L-fucose to the asparagines-linked *N*-acetylglucosamine residue of glycopeptide from α1-acid glycoprotein. Biochem Biophys Res Commun 72:909–916.

Yanagidani S, Uozumi N, Ihara Y, Miyoshi E, Yamaguchi N, Taniguchi N. 1997. Purification and cDNA cloning of GDP-L-Fuc: *N*-acetyl-β-D-glucosaminide: α1-6-fucosyltransferase (α1-6 FucT) from human gastric cancer MKN45 cells. J Biochem 121:329–332.

Zheng H, Wilson JH. 1990. Gene targeting in normal and amplified cell lines. Nature 344:170–173.